

Supporting information of  
**Synthesis of SnO<sub>2</sub>/MoS<sub>2</sub> composites with Different  
Component Ratios and their Applications as Lithium Ion  
Battery Anodes**

*Yu Chen,<sup>a\*</sup> Jia Lu,<sup>b</sup> Shi Wen,<sup>a</sup> Li Lu,<sup>b</sup> and Junmin Xue<sup>a\*</sup>*

<sup>a</sup>Department of Materials Science and Engineering,

National University of Singapore, Singapore, 117576

E-mail: msexuejm@nus.edu.sg, msecheyu@nus.edu.sg

<sup>b</sup>Department of Mechanical Engineering,

National University of Singapore, Singapore, 117576

Sample Name	ICP Measured Value		Calculated Value		Component	
	Sn (wt%)	Mo (wt%)	O (wt%)	S (wt%)	SnO <sub>2</sub> (wt%)	MoS <sub>2</sub> (wt%)
<i>MoS<sub>2</sub></i>	-	55.63	-	37.18	-	92.82
<i>SnO<sub>2</sub>/MoS<sub>2</sub>-1</i>	22.90	36.01	6.17	24.06	29.07	60.06
<i>SnO<sub>2</sub>/MoS<sub>2</sub>-2</i>	33.93	26.53	9.15	17.7	43.08	44.27
<i>SnO<sub>2</sub>/MoS<sub>2</sub>-3</i>	43.79	17.22	11.81	11.51	55.60	28.73
<i>SnO<sub>2</sub>/MoS<sub>2</sub>-4</i>	50.75	9.94	13.68	6.64	64.43	16.58

Figure S1. ICP analysis of atomic percentages of pure MoS<sub>2</sub> and various SnO<sub>2</sub>/ MoS<sub>2</sub> composites.

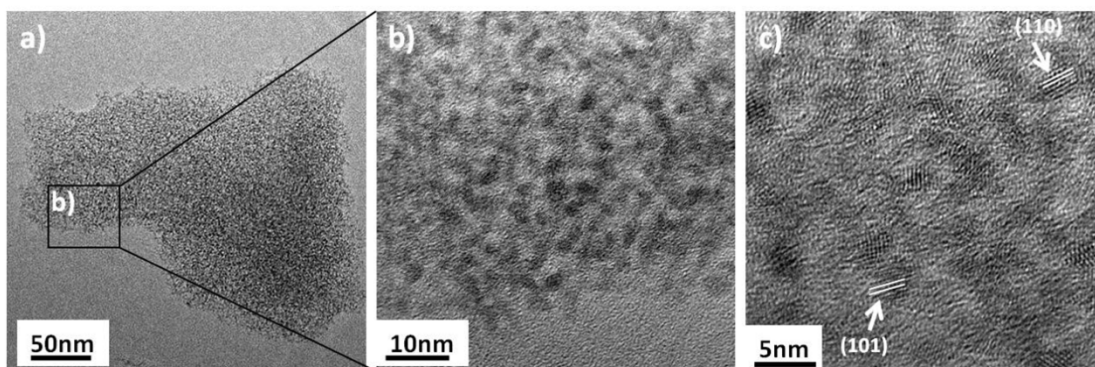


Figure S2. TEM images of SnO<sub>2</sub> nanoparticles under different magnifications.

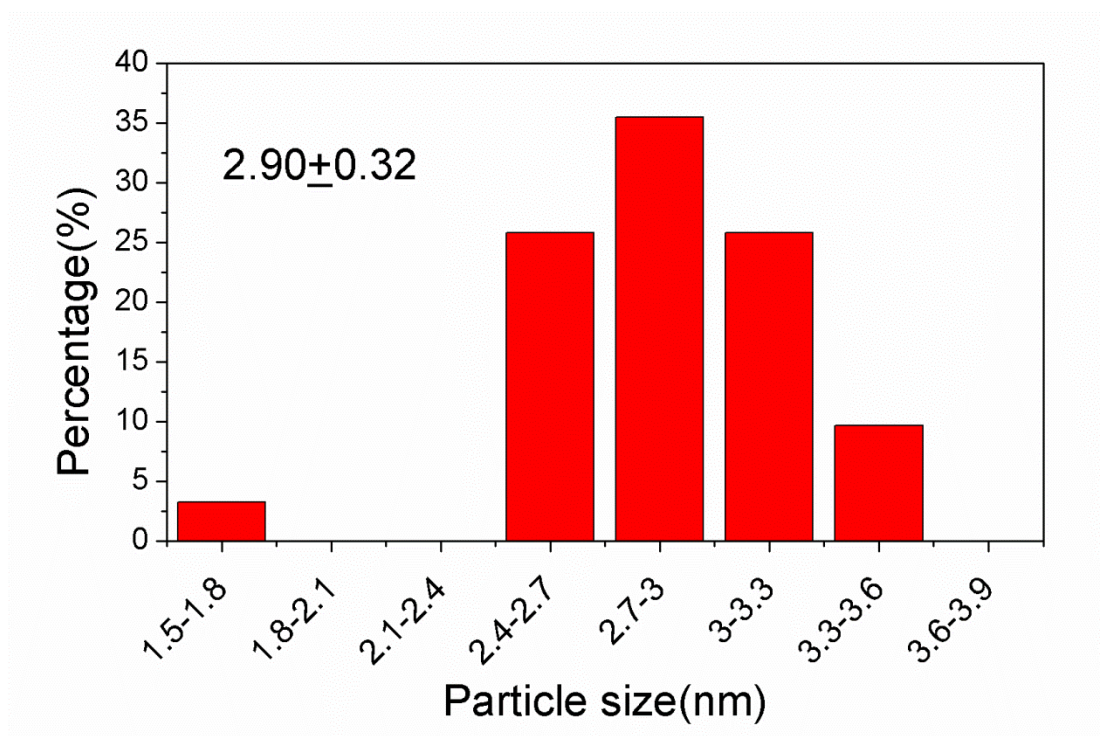


Figure S3. Size distribution of SnO<sub>2</sub> nanoparticles from SnO<sub>2</sub>/MoS<sub>2</sub> composites.

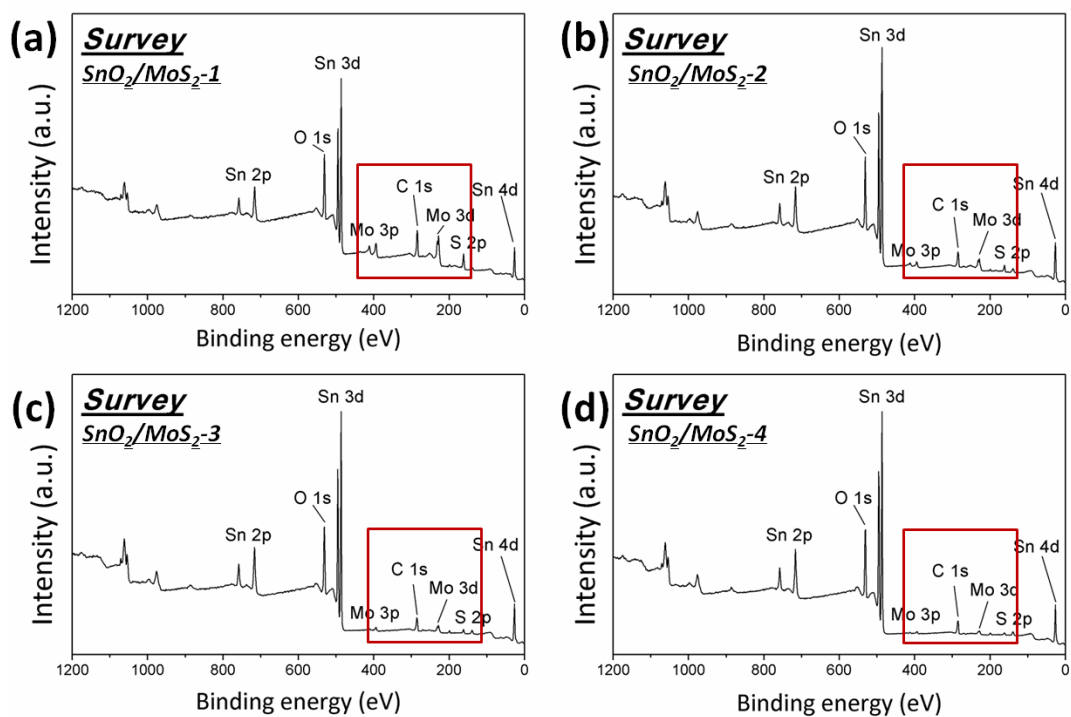


Figure S4. XPS survey spectra of (a)  $\text{SnO}_2/\text{MoS}_2$ -1, (b)  $\text{SnO}_2/\text{MoS}_2$ -2, (c)  $\text{SnO}_2/\text{MoS}_2$ -3, and (d)  $\text{SnO}_2/\text{MoS}_2$ -4.

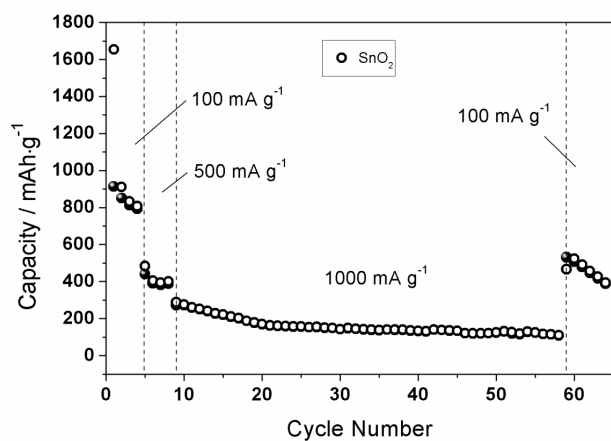


Figure S5. Electrochemical performance of pristine  $\text{SnO}_2$  nanoparticles.

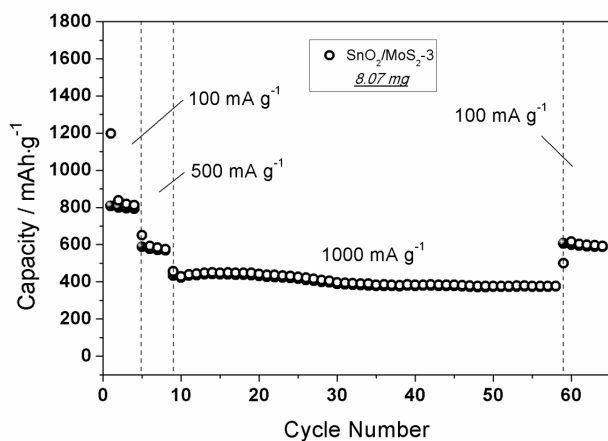


Figure S6. Electrochemical performance of SnO<sub>2</sub>/MoS<sub>2</sub>-3 with high loading amount.

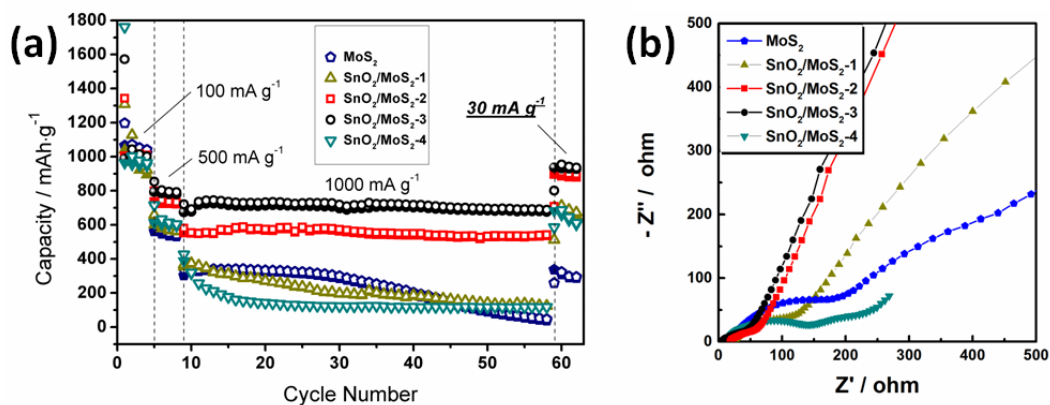


Figure S7 (a) Electrochemical behaviors and (b) corresponding Nyquist plots of all four composites and pure MoS<sub>2</sub> nanosheets when the current density returned to a lower value of 30 mA g<sup>-1</sup> at 59<sup>th</sup> cycle.

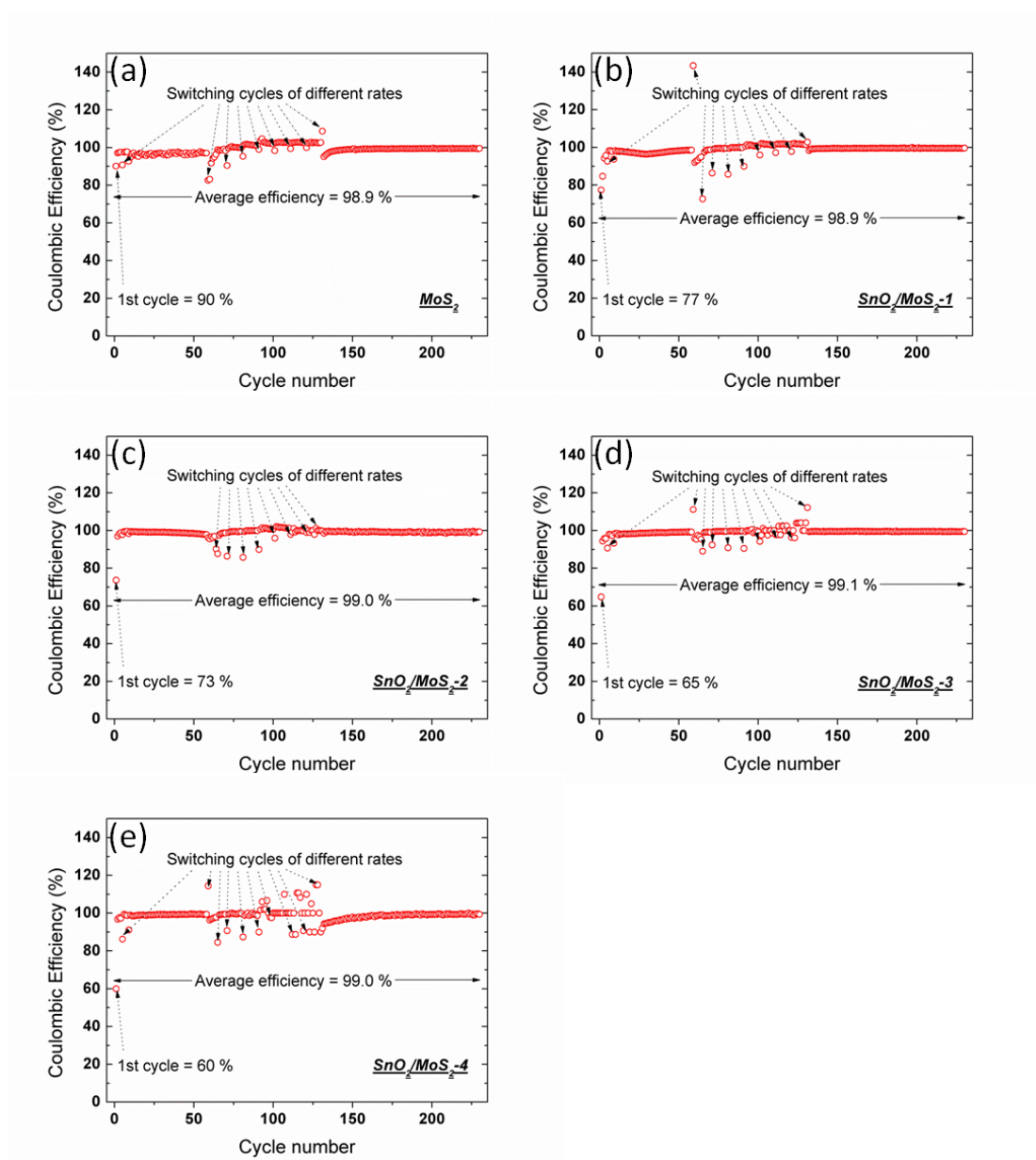


Figure S8. Coulombic efficiencies of a)  $\text{MoS}_2$ , b)  $\text{SnO}_2/\text{MoS}_2$ -1, c)  $\text{SnO}_2/\text{MoS}_2$ -2, d)  $\text{SnO}_2/\text{MoS}_2$ -3, and e)  $\text{SnO}_2/\text{MoS}_2$ -4.

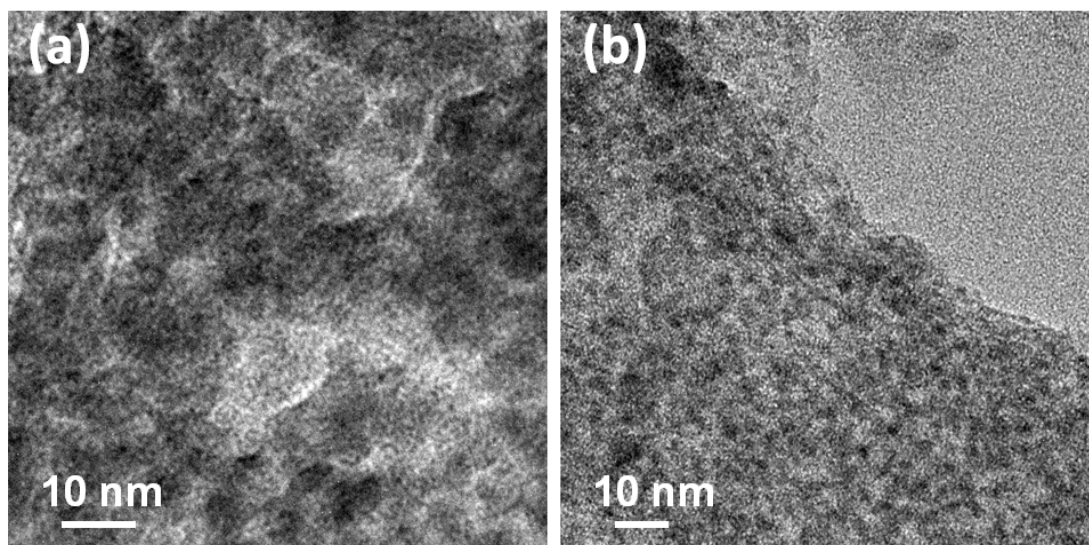


Figure S9. TEM images of (a) MoS<sub>2</sub> nanosheets and (b) SnO<sub>2</sub>/MoS<sub>2</sub>-3 composite after electrochemical tests.

Anodes	SnO <sub>2</sub> /MoS <sub>2</sub> -3	SL-MoS <sub>2</sub> -GNS02	MoS <sub>2</sub> /G/PEO	SnO <sub>2</sub> /G	3D Sn-G
<b>Initial capacity</b> capacity @ current density (mAh g <sup>-1</sup> @mA g <sup>-1</sup> )	979 @100	912 @100	730 @100	978 @67	1081 @293
<b>Rate capability</b> capacity @ current density (mAh g <sup>-1</sup> @mA g <sup>-1</sup> )	658 @1000	571 @1000	500 @1000	400 @1000	460 @879
<b>Cyclic Stability</b> Capacity change (cycle number) @ current density (mAh g <sup>-1</sup> @mA g <sup>-1</sup> )	+18(100) @1000	~-30(55) @100	~-20(5) @1000	-200 (50) @100	+6(4000) @879
Reference	This work	[23]	[33]	[34]	[35]

Figure S10. Comparison of electrochemical performance of SnO<sub>2</sub>/MoS<sub>2</sub>-3 and those of similar works in literature.